ZANCO Journal of Pure and Applied Sciences

TYPE: Original article
DOI http://dx.doi.org/10.21271/ZJPAS.36.6.1

OPEN ACCESS

*Corresponding author

Dlshad H. Hassan
Dlshad.hassan@soran.edu.iq

RECEIVED :04 /09/2024
ACCEPTED :06/10/ 2024
PUBLISHED :31/12/ 2024

KEYWORDS:

PLGA, hyaluronic acid, P53, colorectal carcinoma, drug delivery system, Dactolisib, PI3K/AKT/mTOR pathway, personalized therapy.
.

Evaluation of a Novel PLGA-HA-Based Drug Delivery System Targeting the cell cycle and PI3K/AKT/mTOR Pathway in HCT116 Colorectal Carcinoma Cells with Differing P53 Statuses

Dlshad H. Hassan[1*], Goran Othman[2,3], Esmaeil Babaei[4]

1*Department of Biology, Faculty of Science, Soran University, Soran-Erbil, Iraq
2Department of Medical Laboratory Technology, Erbil Health and Medical Technical College, Erbil Polytechnic University, Kirkuk St., Erbil 44001, Kurdistan Region, Iraq.
3Department of Medical Laboratory Technology, Al-Qalam University College, Kirkuk 36001, Iraq.
4*Department of Biology, School of Natural Sciences, University of Tabriz, Tabriz, Iran

ABSTRACT

Colorectal carcinoma (CRC) is a very important health problem all over the world, and the P53 gene plays an important role in tumor development and in treatment response. The strategy of developing novel DDS that could target specific tumor pathways is one of the most promising approaches to improve therapeutic efficacy. The aim of this study was to evaluate the performance of a newly synthesized PLGA-HA-based DDS encapsulating the mTOR inhibitor Dactolisib on HCT116 CRC cells with differing P53 statuses; P53 positive and P53 negative. The previously synthesized and characterized DDS was tested on HCT-116 P53 positive and negative cell lines. Assessments included: cell cycle distribution analysis by flow cytometry; gene expression profiling of key components of the PI3K/AKT/mTOR pathway by using qPCR, and proteomic via Western blotting. DDS induced a differential effect on the cell cycle progress, which arrested the cell cycle at the G0/G1 phase in a statistically significant way in P53 positive cells, while in P53 negative cells, it resulted in an increase in the S phase. The gene expression analysis revealed downregulation of PIK3CA, AKT1, and MTOR in both cell lines; however, the inhibition seemed more potent in P53-positive cells. The proteomic analysis confirmed reduced p-AKT and p-mTOR with increased levels of P53 protein in P53-positive cells. The new PLGA-HA-based DDS exhibits promising anti-cancer activity against CRC cells, which have different influences related to P53 status. These observations suggest an application for personalized cancer therapy, particularly in the case of tumors with functional P53.

1.Introduction

Colorectal carcinoma is the second leading cause of cancer-related deaths worldwide. There is, therefore, an urgent need for the design and development of new therapeutic approaches which will further improve outcomes in patients affected by this disease (Siegel et al., 2023). Improved chemotherapy notwithstanding, acquired resistance to treatment and recurrence remain common, underscoring the need for targeted therapies that selectively eliminate tumor cells with fewer side effects. Recent advancement in nanotechnology opens up a bright avenue for such site-directed drug delivery system development (DDS) (Kumar et al., 2023).

One of the prime key pathways implicated in CRC is the PI3K/AKT/mTOR pathway. The pathway exhibits a central role in cell growth, proliferation, survival, and metabolic processes with respect to specific signals (Leiphrakpam and Are, 2024). The dysregulation of this pathway is often associated with the development and the progression of diverse cancers, including CRC (Glaviano et al., 2023). Targeting of the PI3K/AKT/mTOR pathway therefore has emerged as a compelling strategy in cancer therapy (Peng et al., 2022). Dactolisib, being a dual inhibitor of PI3K and mTOR, shows considerable anti-cancerous action in preclinical scenarios (Toson et al., 2022). However, its clinical application has been limited by poor bioavailability and systemic toxicity (Sirico et al., 2023).

Nanoparticle-based drug delivery systems have been extensively studied as a means to overcome these limitations (Li et al., 2023). Poly (lactic-co-glycolic acid) (PLGA) is one of the most widely used polymers for nanoparticle synthesis due to its biocompatibility, biodegradability, and ability to provide controlled drug release (Lu et al., 2023). The PLGA-HA-based DDS encapsulating the mTOR inhibitor Dactolisib targets HCT116 CRC cells by leveraging HA's affinity for CD44 receptors, which are overexpressed in cancer cells. This selective targeting enhances drug uptake via receptor-mediated endocytosis. Once inside the cells, the acidic tumor environment and intracellular lysosomal conditions degrade the PLGA matrix, allowing controlled release of Dactolisib. In p53-positive cells, the mTOR inhibition by Dactolisib can enhance p53-mediated apoptotic pathways, while in p53-negative cells, it disrupts cell growth and survival through p53-independent mechanisms, thereby inhibiting tumor progression. (Hou et al., 2022).

Indeed, the tumor suppressor protein p53 plays a critical role in the maintenance of genomic stability through the induction of cell cycle arrest, apoptosis, or senescence in response to DNA damage(Babamohamadi et al., 2022). The TP53 gene is one of the most frequently mutated genes in CRC; moreover, loss of p53 function is strongly associated with poor prognosis and resistance to therapy (Babamohamadi et al., 2022). Consequently, the efficacy of cancer therapies can vary significantly depending on the p53 status of the tumor cells (Marei et al., 2021).

The aim of the present study was to investigate the efficiency of a novel DDS comprising PLGA nanoparticles conjugated with HA and loaded with Dactolisib to target CRC cells with different statuses of p53. Synthesis and characterization of DDS were made as mentioned in our already published article(Dlshad H. Hassan, 2024). Based on this, the hypothesis to be tested was that DDS-mediated targeting of Dactolisib might improve its anticancer efficacy against HCT116 cells, with an emphasis on activity in the usually resistant p53-deficient cells. In trying to test this hypothesis, we conducted several *in vitro* experiments-cell cycle analysis, gene expression, and proteomic assays-to study the effect of DDS on the PI3K/AKT/mTOR pathway and related cellular processes. These studies could surely yield much-needed information about the possibility of this new DDS as targeted therapy for CRC, especially regarding the status of p53 mutation.

2.Materials and Methods

2.1 Synthesis of Drug Delivery System (DDS)

The DDS used in this study was synthesized according to a previously published protocol from our research team. The system was designed such that a PLGA nanoparticle would be conjugated with hyaluronic acid for the

encapsulation of an mTOR inhibitor, Dactolisib, for a targeted delivery into colorectal cancer cells. The synthesis details, therefore, include the preparation of the nanoparticles, encapsulation of the drug, and conjugation with HA, which have been well elaborated in our earlier publication(Dlshad H. Hassan, 2024).

2.2 Cell Culture

The HCT116 colorectal carcinoma cells, both with and without p53 expression, were acquired from the National Cell Bank of Karolinska University-Sweden and cultured in DMEM (Sigma-Aldrich, St. Louis, MO, USA) supplemented with 10% fetal bovine serum (FBS) (Gibco, New York, NY, USA) and 1% penicillin-streptomycin. about 500,000 cells were seeded on each well in 6-well plates The cells were incubated at 37°C in a humidified environment with 5% CO2. For experiments, the cells were seeded into the appropriate culture plates and allowed to adhere overnight prior to treatment with the drug delivery system (DDS) or free Dactolisib.

2.3 Cell Cycle Analysis

To investigate the effects of DDS on cell cycle distribution, HCT116 p53+ve cells were treated with 37.47nm and 107.2 nm of free Dactolisib and DDS respectively for 24 hours and 113nm and 66.91nm for Free drug and DDS respectively for 48hrs. HCT116 p53-ve cells were treated with 238.9nm and 7.05 nm of free Dactolisib and DDS respectively for 24 hours and 102,3nm and 14.93nm for Free drug and DDS respectively for 48hrsAfter the treatment period, the cells were harvested, rinsed with cold PBS, and fixed in 70% ethanol at -20°C overnight. The fixed cells were then stained with propidium iodide (PI) and analyzed using a FACSCanto™ II Flow Cytometer (BD Biosciences, Austria). The data obtained were analyzed using FlowJo software, Version 10, to determine the distribution of cells across the different phases of the cell cycle, including G0/G1, S, and G2/M phases.

2.4 Protein Expression Analysis

Western blotting was utilized to assess the expression of proteins involved in the PI3K/AKT/mTOR signaling pathway. HCT116 cells were treated with DDS or free Dactolisib for 24 and 48 hours, followed by lysis in RIPA buffer. The protein concentrations were determined using the Bradford assay. Equal amounts of protein were then separated via SDS-PAGE and transferred onto PVDF membranes. The membranes were blocked with 5% non-fat dry milk and incubated with primary antibodies specific to the target proteins (All required antibodies were purchased from Santa Cruz Biotechnology Inc.), followed by HRP-conjugated secondary antibodies. Beta-actin was employed as a loading control. The protein bands were visualized using an enhanced chemiluminescence (ECL) detection system.

2.5 Gene Expression Analysis

Quantitative real-time PCR (qRT-PCR) was conducted to measure the expression levels of key genes in the PI3K/AKT/mTOR pathway. Total RNA was extracted from both treated and untreated HCT116 cells using TRIzol reagent, following the manufacturer's protocol. Complementary DNA (cDNA) was synthesized using a reverse transcription kit. qRT-PCR was performed using SYBR Green Master Mix, with beta-actin serving as an internal control to normalize the gene expression levels. Specific primers targeting the genes listed in Table 1 were used for the analysis. Relative gene expression levels were calculated using the 2^-ΔΔCt method.

2.6 Statistical Analysis

All experiments were conducted in triplicate, and data were expressed as mean ± standard deviation (SD). Statistical comparisons between groups were performed using one-way ANOVA followed by post hoc tests. A p-value of <0.05 was considered statistically significant. GraphPad Prism was applied for performing statistical analysis.

3. Results

3.1 Cell Cycle Analysis

Cell cycle distribution of HCT116 cells in different phases like Sub G1, G1, S, and G2 and G2/M was analyzed by flow cytometry following 24 and 48 hours of Dactolisib and Dactolisib-loaded DDS treatment, as shown in Fig. 1A.

Sub G1 Phase (Cells in Sub G1 have undergone apoptosis and display DNA fragmentation,

resulting in less DNA content than normal cells in G1 phase): As shown by cell cycle analysis using flow cytometry, the present study described the influence of Dactolisib and Dactolisib-loaded DDS against HCT 116 cell lines. In the case of HCT 116, +ve P53, no statistical difference in the cell population of Sub G1 was observed between the control group and DDS-treated groups. On the other hand, the Dactolisib-treated group showed a highly significant increase of the Sub G1 cell population, compared to both the control and DDS groups. After 48 hours of treatment, there was no statistical difference between the control and DDS groups, whereas the cell population in the Dactolisib-treated group was decreased, as compared to both control and DDS groups. Fig. 1B.
A different pattern was observed in the distribution of the Sub G1 cell population in HCT 116, -ve P53. At 24 hr treatment, the Dactolisib group increased as compared to the control and DDS groups, while the DDS group showed an increase as compared to the control group. No statistical change in the Sub G1 cell population was observed between the treated groups at 48 hr treatment.

G1 Phase (Cells grow in size, synthesize proteins, and prepare for DNA replication, with normal diploid DNA content): HCT 116, +ve P53P53 cell population in G1 phase after 24 and 48 hr. (Fig. 1C) of treatment was increased significantly in both Dactolisib and DDS treated groups against the control group which showed no change between two treated groups at 24 hr. In remaining treated groups, G1 phase population showed no statistical difference. In the case of HCT 116, -ve P53P53, both treated groups showed a significant increase in cell population at G1 phase compared with the control group after 24- and 48-hour treatments. Again, there is no statistical difference between Dactolisib and DDS-treated groups as in Fig. 1C.

S Phase (Cells are actively synthesizing DNA, leading to a gradual increase in DNA content as replication progresses): The cell population at the S phase in HCT 116, +ve P53 did not differ from the statistical point of view after 24 and 48 hours of treatment. The same pattern was repeated in HCT 116, -ve P53 after 24 and 48 hours of treatment as no significant changes were detected in the cell population of S phase in control, Dactolisib and DDS groups as in Fig. 1D.

G2 Phase (Cells complete DNA replication and prepare for mitosis, containing a fully duplicated genome): In the G2 phase, the cell population of HCT 116, +ve P53 was reduced for both Dactolisib and DDS groups compared to the control group after 24 h of treatment, though there is no significant difference among the two treated groups. No changes were evident in the G2 phase cell population of HCT 116, +ve P53 after 48 hr and in HCT 116, -ve P53 after 24 and 48 hr of treatment (Fig. 1E).
G2/M phase (Cells are in transition between G2 and mitosis, preparing for chromosome condensation and alignment for division): In the case of G2/M phase, cell population HCT116 +ve P53 showed decreased in DDS group as compared to Dactolisib and control group, while in the group treated with dactolisib, cell population didn't vary much as compared to control and DDS. The G2/M phase cell population of HCT 116, +ve P53 did not show any significant difference after 48 hours. Likewise, the HCT 116, -ve P53 did not exhibit any difference after 24 and 48 hours post treatment (Fig. 1F).

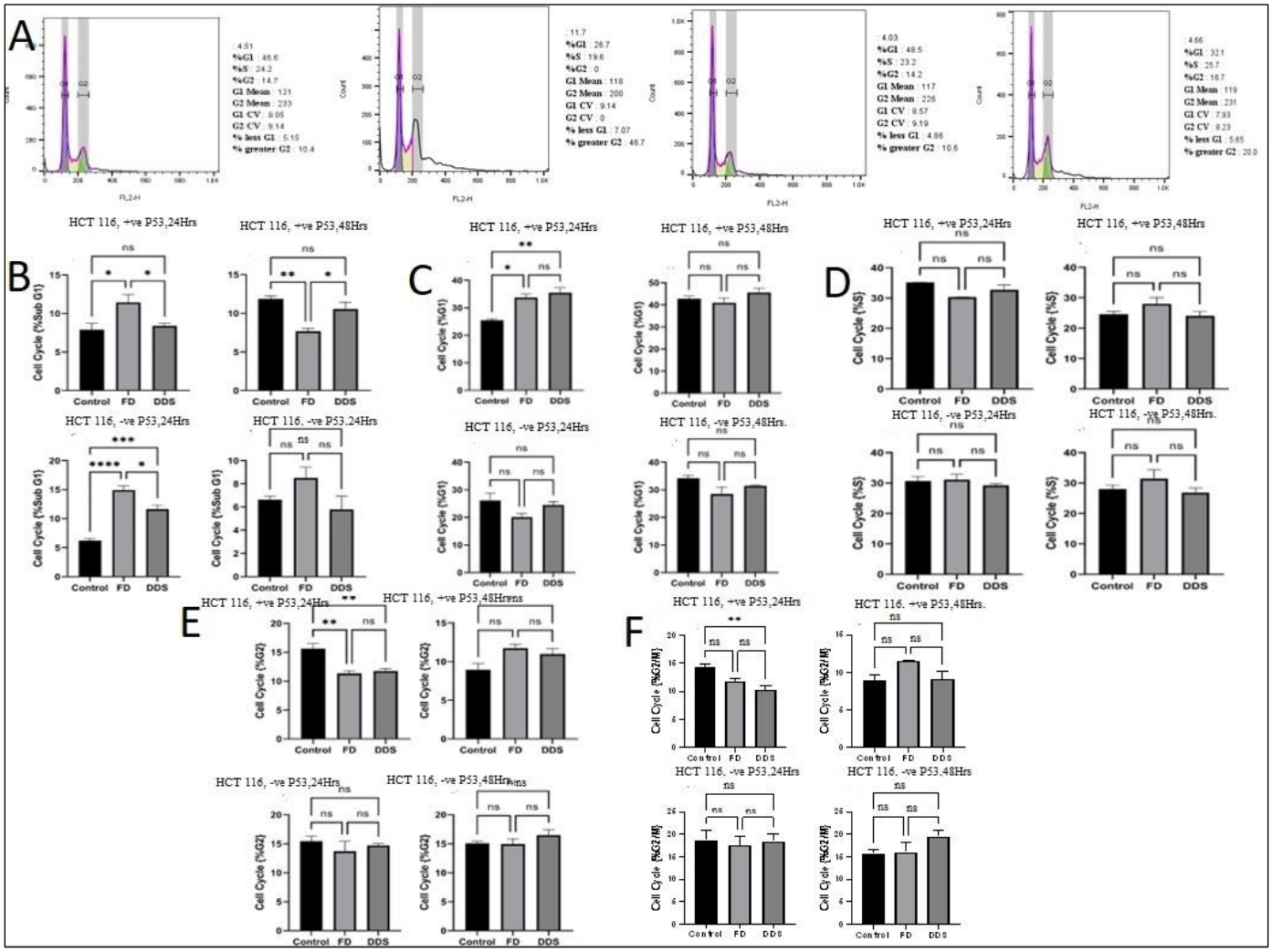

Fig1. Flow cytometric cell cycle analysis of Dactolisib (FD) and the DDS on HCT116.+ve P53 and HCT116-Ve P53 cell lines (A), along with cell population analysis of different cell cycle phases.Following DDS treatment, an increase in the sub-G1 phase (B) was observed, particularly in p53-negative cells, indicating enhanced apoptosis. In the G1 phase (C), there was significant arrest in both p53-positive and p53-negative cells, with a more pronounced effect in p53-negative cells. The S phase (D) population was notably reduced across both groups, suggesting a decrease in DNA synthesis. In the G2 phase (E), p53-positive cells exhibited a slight increase, reflecting some progression through the cell cycle, whereas p53-negative cells remained largely unchanged. In the G2/M phase (F), there was a minor decrease in the p53-negative cell population, indicating early cell cycle arrest, while p53-positive cells remained unaffected.

3.1 Cell Cycle Analysis

The protein expression of p-4E-BP1, 4E-BP1, mtOR, p-S6K, S6K, AKT. After 24 hrs. of treatment, in HCT 116, +ve P53 (Fig. 2A), levels of p-4E-BP1 were reduced in both Dactolisib and DDS groups compared with the control group. The level of 4E-BP1 was reduced in the Dactolisib group, while in the control and DDS groups it remained the same. mTOR protein was significantly reduced in the DDS group when compared to both untreated controls and Dactolisib-treated groups. The p-S6K levels were reduced in both the Dactolisib and DDS groups compared to the control. However, the DDS group showed a higher degree of reduction in the p-S6K level when compared with the Dactolisib group alone. In the Dactolisib-treated group, the S6K was elevated compared with the control, but the DDS group showed an even greater increase in S6K protein expression. Both AKT and its phosphorylated form showed increased expression in treated groups with both Dactolisib and DDS.

In HCT 116, -ve P53 (Fig. 2B), after 24 h treatment, the levels of p-4E-BP1 in the DDS

group were significantly reduced compared with both the control and the Dactolisib-treated group, while the level of 4E-BP1 was increased in the Dactolisib group when compared to the control and the DDS group that showed the highest level. The mTOR protein level was highly reduced in the DDS group when compared with both control and Dactolisib-treated groups. The expression level of p-S6K was lower in the Dactolisib group than in the control, while much higher in the DDS group for p-S6K. In addition, S6K was increased in the Dactolisib group, but it showed the lowest S6K level in the DDS group among the treated groups. The lowest levels of p-AKT and AKT were seen in the DDS group, while AKT levels increased but p-AKT decreased in the Dactolisib group.
HCT 116, +ve P53, following 48 hours of treatment, the levels of p-4E-BP1, 4E-BP1, mTOR, p-S6K, S6K, p-AKT in the Dactolisib-treated group were lower compared to control but higher than that of DDS group. Compared to both the control and DDS-treated groups, the AKT level in the Dactolisib-treated group was low. In HCT 116, -ve P53, the levels of p-4E-BP1, 4E-BP1, p-S6K, p-AKT, and AKT were drastically reduced in the DDS group when compared with the rest of the groups. mTOR protein levels have increased in the Dactolisib group, while the control and DDS groups showed similar levels. S6K was higher in the DDS group compared to the control group; Dactolisib-treated had the highest S6K level.

The ratio of p-AKT/AKT, p-S6K/S6K and p-4E-BP1/4E-BP1 in HCT 116, +ve P53 and HCT 116, -ve P53 (Fig. 2E a&b) after 24 hr treatment were calculated. In the case of the p-AKT/AKT ratio, the value for the DDS group was 0.94 as compared to the control group, 0.92, whereas the highest value expressed by Dactolisib-treated was 1.00. The highest ratios regarding p-S6K/S6K and p-4E-BP1/4E-BP1 were from the control, 1.43 and 1.14; Dactolisib, 1.01 and 1.00; and DDS groups, 0.78 and 0.81 in HCT 116, +ve P53.
In HCT 116, -ve P53, the maximum increase was seen in the p-AKT/AKT ratio in control (0.80), Dactolisib (0.54), and DDS groups (0.24), while the rest of the p-S6K/S6K and p-4E-BP1/4E-BP1 showed a maximum increase in the control (0.63 and 0.88), Dactolisib (0.41 and 0.74), and DDS groups (0.34 and 0.37). In HCT 116, +ve P53, p-AKT/A. The p-S6K/S6K ratio was highest in the Dactolisib group, at 1.22, followed by the DDS group, at 0.82. For p-4E-BP1/4E-BP1, the control, Dactolisib, and DDS groups obtained the ratios of 0.96, 1.14, and 2.20, respectively. In HCT 116, -ve P53, the p-AKT/AKT ratio dropped in both the control (0.57), Dactolisib (0.45), and DDS groups to 0.44. A p-S6K/S6K ratio decreased in the control to 1.09 and. The p-4E-BP1/4E. (Fig. 2F a&b).

3.3 Gene Expression Analysis

The relative gene expression of mTOR, AKT, 4E-BP1, and S6K genes as represented in Fig. 3 was assessed after 48 hours of treatment. HCT116, p53+ve Cells: mTOR expression in DDS group was significantly reduced as compared to control, while AKT gene expression significantly increased in both Dactolisib and DDS groups. 4E-BP1 expression increased in Dactolisib group while did not change in DDS group. S6K gene expression significantly increased in both the treatment groups as compared to control (Fig 3C a,b,c,&d). HCT116, p53-ve Cells: Compared to control, both Dactolisib and DDS groups had significantly higher gene expressions of mTOR, AKT, and S6K. There is no statistical difference in 4E-BP1 expression between control and DDS groups. However, the Dactolisib group showed a significant increase. (Fig 3D a,b,c,&

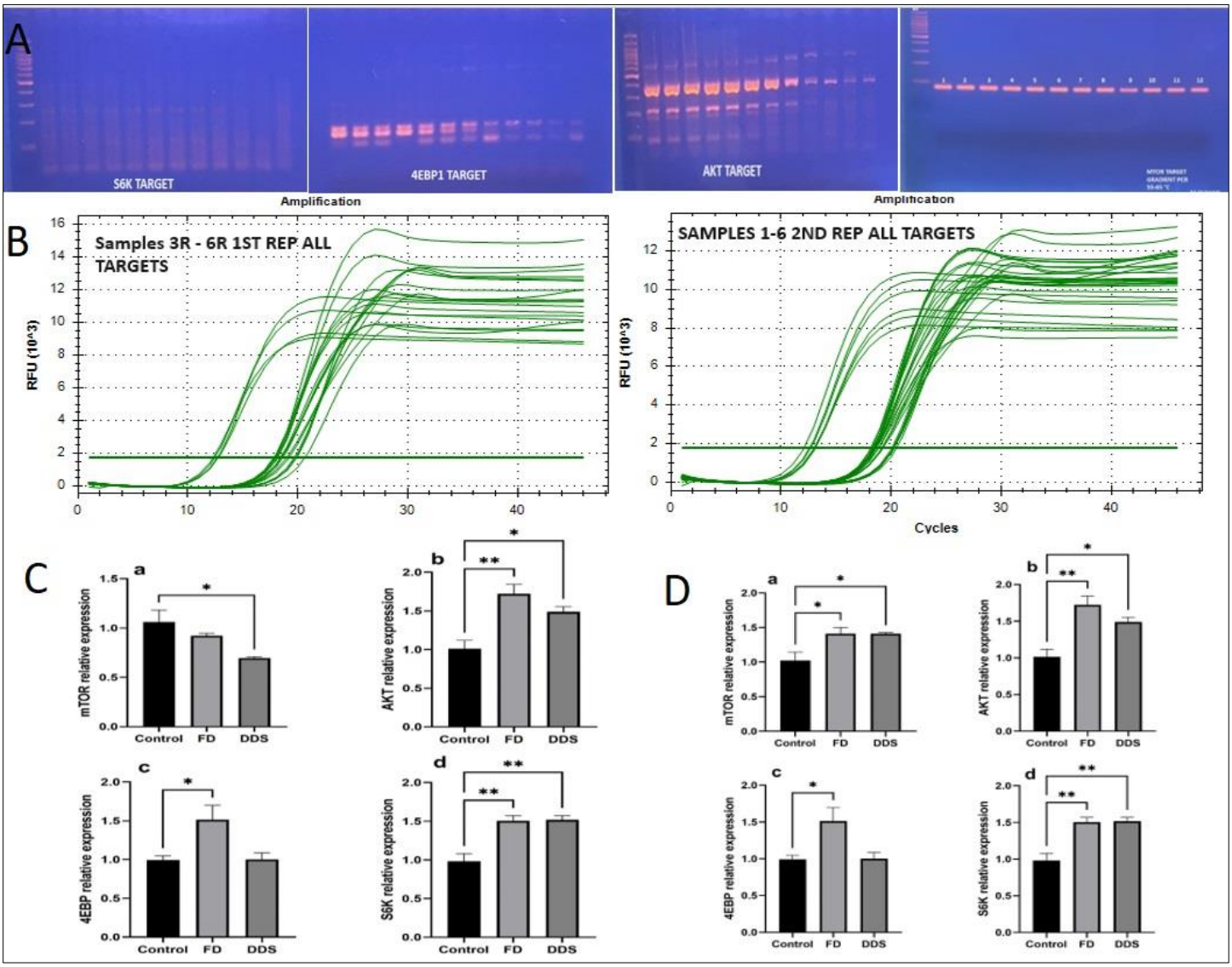

Fig 2. The combined effects of Dactolisib and Dactolisib-loaded DDS on protein expression in HCT116 cells with both +ve and -ve p53 status were assessed after 24 and 48 hours. After 24 hours, in HCT116 +ve p53 cells (A), p-4E-BP1 and mTOR levels were reduced in both treated groups, with a more pronounced decrease in the DDS group, while p-S6K levels declined, and S6K and AKT levels increased, particularly in DDS-treated cells. In HCT116 -ve p53 cells (B), DDS treatment caused a significant reduction in p-4E-BP1 and mTOR, with the lowest p-S6K and AKT levels observed in the DDS group, whereas 4E-BP1 was highest in the DDS group. After 48 hours, in HCT116 +ve p53 cells (C), both treatments led to a reduction in p-4E-BP1, mTOR, p-S6K, and p-AKT levels, with AKT being higher in the DDS group. In HCT116 -ve p53 cells (D), DDS treatment resulted in the lowest p-4E-BP1, 4E-BP1, p-S6K, and p-AKT levels, while mTOR and S6K were higher in the Dactolisib-treated group. Regarding protein ratios after 24 hours (E), the p-AKT/AKT ratio was highest in Dactolisib-treated cells, while in -ve p53 cells, DDS-treated cells showed the lowest ratios for all proteins. After 48 hours (F), p-AKT/AKT and p-S6K/S6K ratios were lowest in DDS-treated cells, while the p-4E-BP1/4E-BP1 ratio was highest in DDS-treated groups**.**

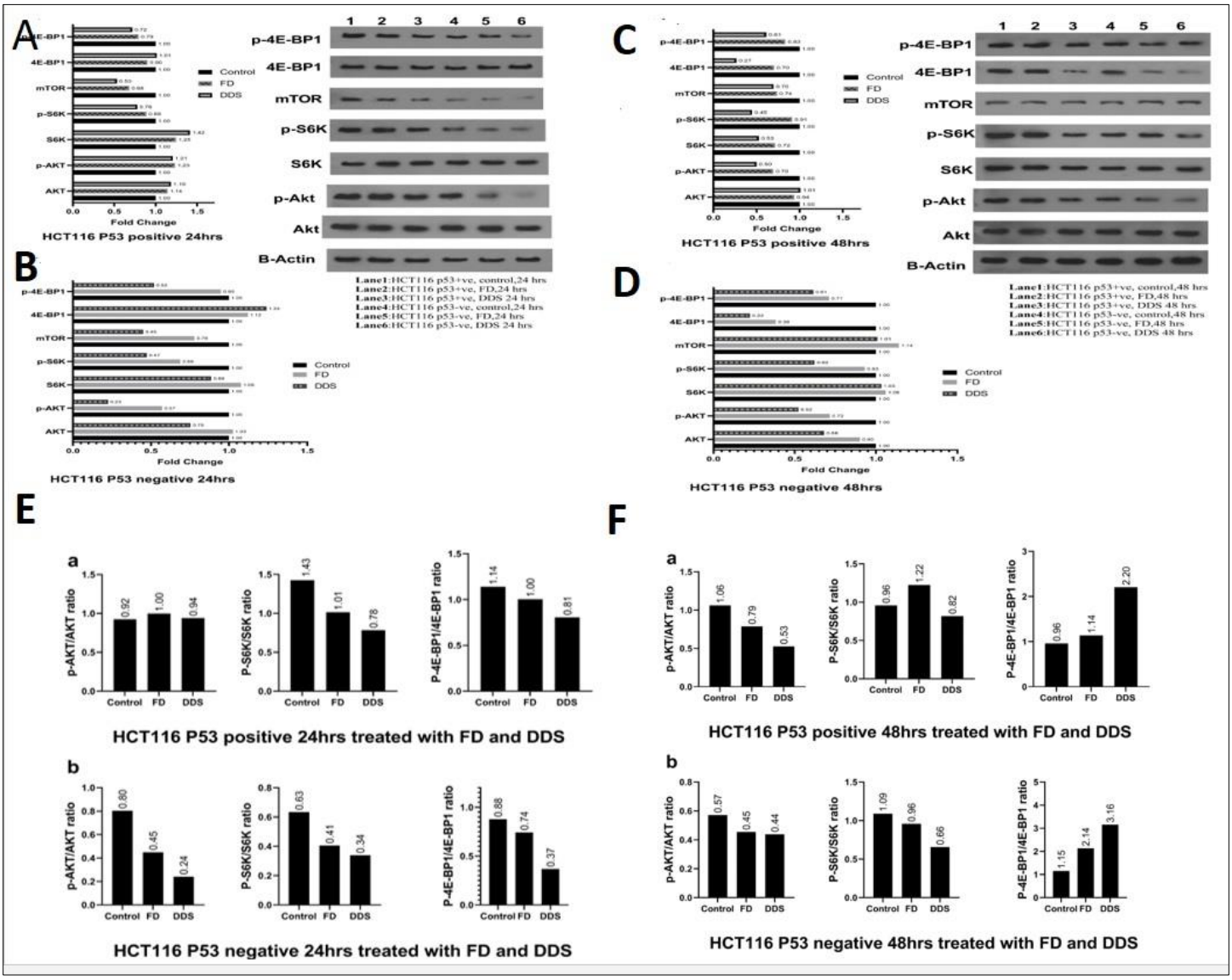

Fig 3. The relative gene expression of *mTOR*, *AKT*, *4E-BP1*, and *S6K* in HCT116 +ve (C) and -ve (D) p53 cells after 48 hours of treatment with Dactolisib (FD) and DDS. In +ve p53 cells, *mTOR* decreased significantly in DDS, *AKT* increased in both treatments, *4E-BP1* rose in FD but remained stable in DDS, and *S6K* increased in both. In -ve p53 cells, *mTOR*, *AKT*, and *S6K* increased in both treatments, while *4E-BP1* increased only in FD. Gel electrophoresis of PCR products (A) and RT-QPCR curves of targeted genes (B) are provided, offering insights into the transcriptional regulation of key genes involved in cellular processes affected by the treatments.

4. Discusion

The results of this study provide deep insight into how Dactolisib and Dactolisib-loaded DDS affect cell cycle and proteomic profile changes in HCT 116 cell lines with different P53 statuses. The differential response observed with HCT 116, +ve P53, and -ve P53 cells bears out the significance of P53 in mediating cellular responses to treatments aimed at the mTOR pathway.

In the Sub G1 phase, in the Dactolisib-treated group of the HCT 116, +ve P53 cells, there was an observed increase in cell population after 24 hours of treatment and highly significant increase of the Sub G1 cell population, compared to both the control and DDS groups in p53 positive cells. This, in turn, would imply that Dactolisib acts via apoptosis induction and would thus explain the earlier observations on the possibility of cell death following mTOR inhibition in wild-type P53-expressing tumor cells (Zou et al., 2020).

Interestingly, no such increase was found for the DDS group; this may be indicative of a different modulation of the apoptotic response by DDS through various drug release kinetics or by interaction with cell uptake mechanisms (Yoon, 2020).

Further, the results at the G1 phase showed a high increase in the cell population of both the treated groups, pointing out G1 arrest as one of the most important modes of action for Dactolisib. This arrest is consistent with the known role of mTOR in regulating cell cycle progression through the G1 phase (Dowling et al., 2010). In agreement with this hypothesis, there was no significant difference between the Dactolisib and DDS groups, suggesting that DDS effectively delivers the drug while the timing and intensity of G1 arrest may be similar to that elicited by free Dactolisib.

In contrast, in the case of the S phase, no significant differences were determined in all treatments, suggesting that DNA synthesis is not very much affected by the interventions applied. might be beneficial because stability in the S phase means that the principal impacts of Dactolisib and its DDS formulation remain on other aspects of the cycle, thus better minimizing effects that would cause harm rather than good (Eastman, 2004).

Most importantly, the G2 phase results, especially regarding cell population reduction in both treated groups, evidence that Dactolisib impacts cell cycle checkpoints. Previous studies have confirmed that mTOR inhibition causes G2 phase arrest by disrupting the PI3K/AKT/mTOR signaling pathway, preventing cells from entering mitosis. No significant difference between the treated groups leads to the assumption that DDS maintains the aptitude of a drug to induce G2 arrest and thus has the potential to act as an effective delivery system (Patra et al., 2023).

The G2/M phase results are particularly notable, showing a significant reduction in the DDS-treated group compared to the control and Dactolisib-treated groups. This suggests that the DDS formulation enhances the arrest of cells at the G2/M transition. The mechanism likely involves the more efficient and sustained release of Dactolisib, leading to prolonged inhibition of the PI3K/AKT/mTOR pathway. This inhibition disrupts the activation of key regulators such as Cyclin B and Cdk1, preventing the progression from G2 to M phase. As a result, the DDS improves drug delivery, enhancing the timing and extent of cell cycle arrest. (Yakkala et al., 2024).

Proteomic analysis would further elucidate the molecular processes that influence such changes in the cell cycle. Indeed, lower levels of p-4E-BP1, mTOR, and p-S6K in the treated groups-notably in the DDS group-are in concert with suppression of the mTOR pathway, which is important in the regulation of cell growth and proliferation (Thoreen et al., 2012). This would suggest that the rise in AKT and p-AKT levels observed in some of the treatment groups represents a compensatory response, since feedback activation of the PI3K/AKT pathway after mTOR inhibition is a well-documented phenomenon (Rascio et al., 2021).

The differential sensitizing effects observed among HCT 116, +ve P53, and -ve P53 cells indicate the importance of P53 status in the determination of cellular responses to mTOR inhibition. It is well documented that P53 plays a key role in the regulation of the cell cycle and apoptosis, and its presence or absence may importantly affect treatment outcome (Munro et al., 2005, Michel et al., 2021). The proteomic profile differences between the two cell lines may suggest that the Dactolisib DDS formulation modulates activity depending on the genetic background of the cancer cells and possibly could have applications in personalized medicine.

Conclusions

This study demonstrates that Dactolisib, delivered either as a free drug or via a DDS, significantly impacts the cell cycle and proteomic landscape of HCT 116 cell lines. The observed differences between the P53 positive and negative cell lines highlight the complexity of targeting the mTOR pathway in cancer treatment. The DDS formulation shows promise in modulating drug delivery, potentially enhancing therapeutic outcomes. Further research are warranted to explore the mechanisms underlying these effects and to optimize DDS formulations for clinical applications.

Acknowledgment: Not applicable.

Financial support: No financial support.

Potential conflicts of interest. All authors report no conflicts of interest relevant to this article.

References

BABAMOHAMADI, M., BABAEI, E., AHMED SALIH, B., BABAMOHAMMADI, M., JALAL AZEEZ, H. & OTHMAN, G. J. F. I. M. B. 2022. Recent findings on the role of wild-type and mutant p53 in cancer development and therapy. 9**,** 903075.

DLSHAD H. HASSAN, G. O., ESMAEIL BABAEI 2024. Synthesis And Characterization Of Novel PLGA And HA-Based Nanoparticle Drug Delivery System Incorporating Dactolisib And ItsIn VitroEvaluation Against HCT116 Colorectal Carcinoma Cells. *African Journal of Biomedical Research,* 27**,** 1178-1183.

DOWLING, R. J., TOPISIROVIC, I., FONSECA, B. D., SONENBERG, N. J. B. E. B. A.-P. & PROTEOMICS 2010. Dissecting the role of mTOR: lessons from mTOR inhibitors. 1804**,** 433-439.

EASTMAN, A. J. J. O. C. B. 2004. Cell cycle checkpoints and their impact on anticancer therapeutic strategies. 91**,** 223-231.

GLAVIANO, A., FOO, A. S., LAM, H. Y., YAP, K. C., JACOT, W., JONES, R. H., ENG, H., NAIR, M. G., MAKVANDI, P. & GEOERGER, B. J. M. C. 2023. PI3K/AKT/mTOR signaling transduction pathway and targeted therapies in cancer. 22**,** 138.

HOU, X., ZHONG, D., CHEN, H., GU, Z., GONG, Q., MA, X., ZHANG, H., ZHU, H. & LUO, K. J. C. P. 2022. Recent advances in hyaluronic acid-based nanomedicines: Preparation and application in cancer therapy. 292**,** 119662.

KUMAR, A., GAUTAM, V., SANDHU, A., RAWAT, K., SHARMA, A. & SAHA, L. J. W. J. O. G. S. 2023. Current and emerging therapeutic approaches for colorectal cancer: A comprehensive review. 15**,** 495.

LEIPHRAKPAM, P. D. & ARE, C. J. I. J. O. M. S. 2024. PI3K/Akt/mTOR Signaling Pathway as a Target for Colorectal Cancer Treatment. 25**,** 3178.

LI, X., LIU, J., CHEN, H., CHEN, Y., WANG, Y., ZHANG, C. Y. & XING, X.-H. J. G. C. E. 2023. Multi-functional engineered polypeptide-based drug delivery systems for improved cancer therapy. 4**,** 173-188.

LU, Y., CHENG, D., NIU, B., WANG, X., WU, X. & WANG, A. J. P. 2023. Properties of poly (lactic-co-glycolic acid) and progress of poly (lactic-co-glycolic acid)-based biodegradable materials in biomedical research. 16**,** 454.

MAREI, H. E., ALTHANI, A., AFIFI, N., HASAN, A., CACECI, T., POZZOLI, G., MORRIONE, A., GIORDANO, A. & CENCIARELLI, C. J. C. C. I. 2021. p53 signaling in cancer progression and therapy. 21**,** 703.

MICHEL, M., KAPS, L., MADERER, A., GALLE, P. R. & MOEHLER, M. J. C. 2021. The role of p53 dysfunction in colorectal cancer and its implication for therapy. 13**,** 2296.

MUNRO, A., LAIN, S. & LANE, D. J. B. J. O. C. 2005. P53 abnormalities and outcomes in colorectal cancer: a systematic review. 92**,** 434-444.

PATRA, D., BHAVYA, K., RAMPRASAD, P., KALIA, M., PAL, D. J. A. I. P. C. & BIOLOGY, S. 2023. Anti-cancer drug molecules targeting cancer cell cycle and proliferation. 135**,** 343-395.

PENG, Y., WANG, Y., ZHOU, C., MEI, W. & ZENG, C. J. F. I. O. 2022. PI3K/Akt/mTOR pathway and its role in cancer therapeutics: are we making headway? 12**,** 819128.

RASCIO, F., SPADACCINO, F., ROCCHETTI, M. T., CASTELLANO, G., STALLONE, G., NETTI, G. S. & RANIERI, E. J. C. 2021. The pathogenic role of PI3K/AKT pathway in cancer onset and drug resistance: an updated review. 13**,** 3949.

SIEGEL, R. L., WAGLE, N. S., CERCEK, A., SMITH, R. A. & JEMAL, A. J. C. A. C. J. F. C. 2023. Colorectal cancer statistics, 2023. 73**,** 233-254.

SIRICO, M., D'ANGELO, A., GIANNI, C., CASADEI, C., MERLONI, F. & DE GIORGI, U. J. C. 2023. Current state and future challenges for PI3K inhibitors in cancer therapy. 15**,** 703.

THOREEN, C. C., CHANTRANUPONG, L., KEYS, H. R., WANG, T., GRAY, N. S. & SABATINI, D. M. J. N. 2012. A unifying model for mTORC1-mediated regulation of mRNA translation. 485**,** 109-113.

TOSON, B., FORTES, I. S., ROESLER, R. & ANDRADE, S. F. J. P. R. 2022. Targeting Akt/PKB in pediatric tumors: A review from preclinical to clinical trials. 183**,** 106403.

YAKKALA, P. A., NAAZ, F., SHAFI, S. & KAMAL, A. J. E. O. O. T. T. 2024. PI3K and tankyrase inhibitors as therapeutic targets in colorectal cancer. 28**,** 159-177.

YOON, M.-S. J. I. J. O. N. 2020. Nanotechnology-based targeting of mTOR signaling in cancer. 5767-5781.

ZOU, Z., TAO, T., LI, H., ZHU, X. J. C. & BIOSCIENCE 2020. mTOR signaling pathway and mTOR inhibitors in cancer: progress and challenges. 10**,** 31.